

Fabrication and characterization of hydroxyapatite/collagen bone-like nanocomposite through a self-assembly method

Zhenlin Wang^{1,2,*}, Yuhua Yan² and Tao Wan²

¹School of Materials Science and Engineering, Chongqing University of Technology, Chongqing, 400054, China, e-mail: wzl@cqut.edu.cn

²Research Centre of Biomaterials and Engineering, Wuhan University of Technology, Wuhan, 430070, China

* Corresponding author

Abstract

Based on a self-assembly mechanism, a co-precipitation method was utilized to fabricate bone-like biomimetic nanocomposite with a simplified preparation approach and accessible materials to investigate in depth some characteristics of hydroxyapatite/collagen (HAp/Col) nanocomposite for the elucidation of performances in some respects. The as-prepared composite was characterized by X-ray diffraction, scanning electron microscopy, transmission electron microscopy, Fourier transformation infrared spectroscopy, and thermal analysis. The results show that HAp nanocrystals formed as preferentially oriented slender needles 50–100 nm in length on a felt-like Col matrix which is composed of large numbers of randomly oriented Col fibers and showed polycrystalline behavior. The as-prepared cellular composites are analogous in both composition and nanostructured architecture to native bone, longer aging time promotes the growth and purification of nano-HAp on Col, and characterization confirms that chemical interaction occurs and causes intimate bonding between HAp and Col.

Keywords: biomineralization; bone-like; hydroxyapatite/collagen; nanocomposite; self-assembly.

1. Introduction

Hydroxyapatite (HAp) ceramics have been suggested for bone regeneration. From a bone perspective, they exhibit excellent biocompatibility due to their chemical and structural similarity to the mineral phase of native bone. However, clinical applications for tissue engineering have been limited because of their brittleness, difficulty of shaping for implantation, and because new bone formed in a porous HAp network cannot sustain the mechanical loading needed for remodeling. In addition, problems also exist in that it is difficult to control its degradation rate [1, 2]. In addition to HAp, collagen (Col) is one of the two major components of bone. It makes up 89% of the organic matrix and 32% of the volumetric composition of bone. As such, it has significant potential for culturing cells

to produce bone [2]. Col, as a natural polymer, is increasingly being used as a device material in tissue engineering and repair. It is, for example, found in bone (type-I), cartilage (type-II), and in blood vessel walls (type-III) and has excellent biocompatible properties. Col is easily degraded and absorbed by the body and allows good attachment to cells. However, its mechanical properties are relatively low in comparison to bone and it is therefore highly crosslinked or found in composites. The ductile properties of Col help to increase the poor fracture toughness of HAp, combining both Col and HAp should provide an advantage over other materials for use in bone tissue repair [1].

As with all organs in the body, bone tissue has a hierarchical organization over length scales that span several orders of magnitude from the macroscale to the nanostructured (extracellular matrix or ECM) components. Bone ECM comprises both a non-mineralized organic component (predominantly type-I Col) and a mineralized inorganic component (composed of 4 nm thick plate-like carbonated apatite minerals) [3]. The formation of native bone involves a gradual biomineralization process relating to self-assembly, which is ubiquitous in nature at both macroscopic and microscopic scales, and describes the spontaneous association and organization of numerous individual entities into coherent and well-defined structures without external instruction [4]. Bone creation through self-assembly consists of two aspects, one is the hierarchical self-assembly of Col, type-I Col assembly *in vitro* involves formation of a critical subunit approximately 4 nm wide that grows laterally in discrete 4 nm steps by fusion and longitudinally into fibrils via lysine derived crosslinks; and the second represents the oriented array of nano-HAp produced by spontaneous mineralization of calcium phosphate ions using Col as templates through molecular recognition. Inspired by the formation mechanism of native bone as well as the effects of the particular ultrastructure on the enviable properties, researchers recognized it would be desirable to mimic both the composition and structure of native bone for synthetic bone graft substitutes. The biomineralization process through self-assembly as a HAp/Col preparation approach has been the focus of much attention in recent years [5–9]. The HAp/Col composites resembling bone synthesized by biomimetic strategy show great promise in clinical application because of its compositional and partly structural analogy to native bone. In this study, based on a self-assembly mechanism a co-precipitation method was utilized to fabricate bone-like biomimetic nanocomposite with a simplified fabrication approach and accessible materials to investigate in depth some characteristics of HAp/Col nanocomposite for elucidation in some respects that still remain obscure and even controversial.

2. Experimental

2.1. Preparation of HAp/Col bone-like composite

Pure rat tail type-I Col can be easily prepared by the acid leaching method, which has been routinely adopted by peer researchers [10, 11]. Rat tail tendon Col was extracted from four frozen albino rat tails. The skin was removed and the tendon was isolated from other tissues. Tendon fibers were washed with 70% alcohol solution, finely cut and rinsed with deionized water. Then, the fine rat tail tendon fibers were immersed in 1000 ml 0.5 mol/l acetic acid for 3–4 days at 4°C. The telopeptide was removed by pepsin treatment, 200 ml 0.1 mol/l NaOH solution was added and Col fibers precipitated, the mixture was centrifuged at 1645×g by transferring 8 g solution into each tube as a batch and precipitate was collected and then freeze-dried.

An aqueous suspension was made by ultrasonication of 4.46 g finely grounded CaO powder in distilled water and was transferred completely to a tap funnel, 2 g freeze-dried rat tail tendon Col was dissolved in 400 ml 0.15 mol/l acetic acid, 5.4 ml H_3PO_4 was added and thoroughly stirred; the mixture was transferred to another tap funnel. Both solutions were titrated dropwise through respective tap funnels into a central reaction vessel with 1000 ml distilled water previously added and vigorously stirred. The reaction temperature was controlled by a thermostatic water bath and the pH of the reaction solution by a set of pH meters. The temperature was set at 40°C and pH at 9; the resultant products were aged for 12 h, 24 h, and 48 h, and were denoted as HAp/Col-12, HAp/Col-24, and HAp/Col-48, respectively; the supernatant was removed and the precipitation was repeatedly washed with deionized water, and then suction-filtrated and naturally dried at room temperature.

2.2. Characterizations of HAp/Col composite

Phase structure of the composites was characterized by an X-ray diffraction (XRD) meter (D/MAX-III A) using $CuK\alpha$ radiation. A proportion of the slurry obtained by ultrasonication of HAp/Col-48 with deionized water was scooped on a copper mesh to observe microstructure features via transmission electron microscopy (TEM) (H-600STEM/EDXPV9100). Morphology of the composite was observed with a JSM-5610 LV scanning electron microscope (SEM). Chemical interaction between HAp and Col was analyzed with Fourier transformation infrared (FT-IR) measurements with a NICOLET 60SXBFTIR Fourier transform infrared spectrometer, and background noise was corrected with pure KBr data. The organic content and thermal properties were measured by a NETZSCH STA449C thermogravimetric analyzer (TGA) using Al_2O_3 crucible in nitrogen flow and a heating ramp rate of 10 K/min.

3. Results

3.1. Phase analysis of HAp/Col composites

Figure 1 presents the results of XRD measurements on the as-prepared HAp/Col nanocomposites aged for various times.

Several HAp characteristic peaks were observed in the specimen by comparing the standard HAp patterns (Figure 1D; PDF#01-1008). The XRD pattern is highlighted by a higher intensity for the (211) peak compared to the intensity of the other peaks characteristic to HAp. This result can be attributed to a preferential growth of the HAp crystals in the (211) direction due to Col influence [12]. As the HAp peaks of the composite were broad and overlapped with much weaker intensities compared to the standard HAp XRD peaks, it is considered that the grown HAp crystals had low crystallinity or small crystallite size which was similar to inorganic phase of native bone. The cause is thought to arise from the incorporation of impurities, such as carbonate, sodium, and magnesium ions, and non-stoichiometry of the biogenic mineral [13]. Carbonate ion increases HAp solubility and inhibits HAp crystal growth [9]. Longer aging for HAp/Col gives the peaks higher intensities implying a higher crystallization and purity of HAp, correspondingly shorter aging results in poor crystallization and creates a more apatite impurity phase because the short aging contracts the growth of the HAp nucleus, and thus hindered the yielding of HAp crystallites. The sample HAp/Col-12 is measured to be a nearly amorphous substance, some researchers argue that HAp forms by the deposition of an amorphous calcium phosphate (ACP) precursor which is considered as actually “paracrystalline” mineral (i.e., a loss of long-range crystalline order as a result of lattice imperfections) [13], a longer aging duration is assumed to promote the growth and oriented alignment of HAp. Steady temperature, pH value, and Ca^{2+} and PO_4^{3-} ion concentrations facilitate the HAp heterogeneous and epitaxial nucleation on the Col molecules [9], a longer aging implies stable reaction condition for the biomineralization of Col.

3.2. Morphology of HAp/Col composite

The SEM images of HAp/Col composite are shown in Figure 2. Figure 2A presents a graphic with a lower

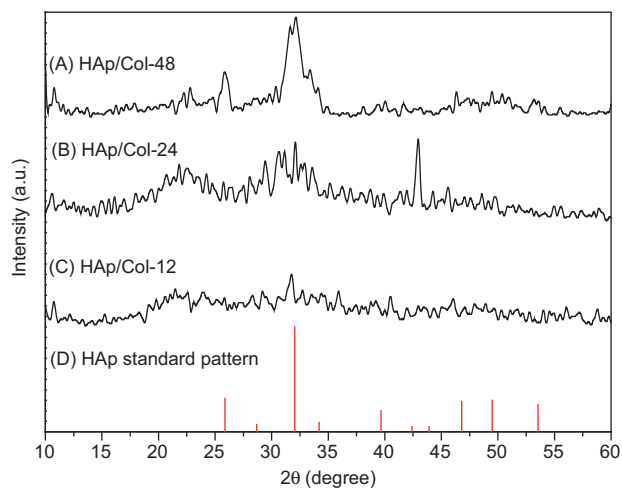


Figure 1 XRD patterns of HAp/Col composites with varied aging time: (A) 48 h; (B) 24 h; (C) 12 h; (D) HAp standard pattern.

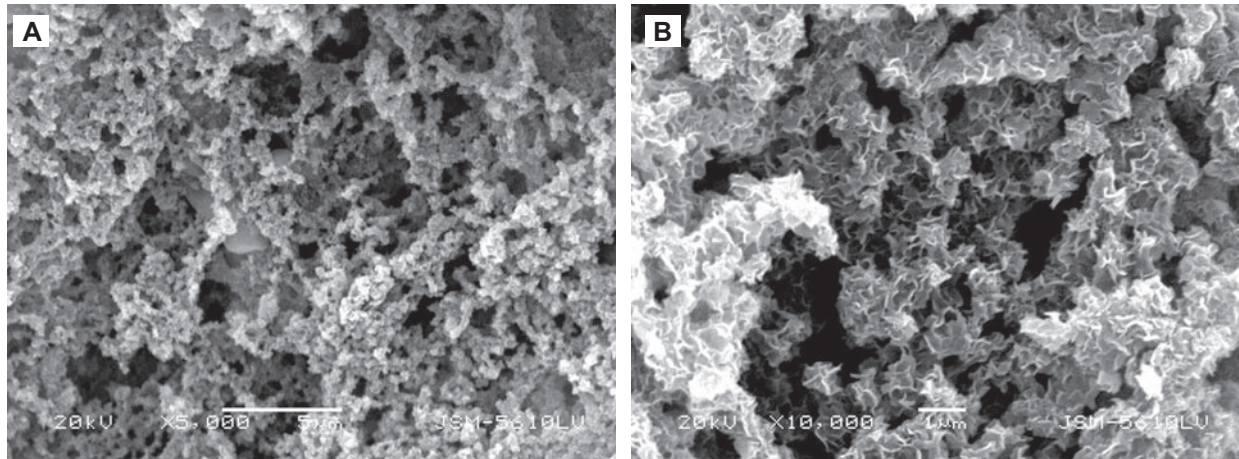


Figure 2 SEM images of as-prepared HAp/Col composite (sample HAp/Col-48). (A) Surface morphology with a lower magnification; (B) cross-sectional fracture morphology at a higher magnification.

magnification showing a hybrid porous structure formed by crosslinking and aggregating of Col matrix with HAp crystallites uniformly adhered to it, the expressed cross-sectional fracture morphology at a higher magnification in Figure 2B further demonstrates that the mineralized fine crystallites bonded to the fibrous bioorganic substance yielding an organic/inorganic complex. It convincingly demonstrates that mineralized Col molecules, 300 nm, in known length self-assembled to be fibrils, which further crosslinked to microfibrils approximately 100 nm in diameter; these microfibrils are arranged into higher level mineral containing Col fibrous bundles 1–4 µm in length. As shown in Figure 2B, the hierarchical hybrid gives the composite peculiar properties, for instance, improved ductibility when compared to singular HAp. The cellular architecture of the as-prepared HAp/Col was constructed through the dehydration of filter cake, this type of structure is similar to that of native bone and facili-

tates the ingrowths and reconstruction of bone tissue after implantation.

3.3. Microstructure of HAp/Col composite

TEM analysis (Figure 3A) shows that HAp crystals formed as slender needles 50–100 nm in length embedded in Col matrix and its (002) electron diffraction (Figure 3B) indicated not single crystalline diffraction behavior but normal pattern of HAp polycrystals, although it is generally accepted that HAp is regularly aligned along the Col fibers with its crystalline c-axis preferentially oriented. This result supports the concept [14] that HAp crystals formed on a Col felt, which is composed of large numbers of randomly oriented Col fibers. The electron diffraction did not show the arching pattern but showed the same ring patterns as the normal pattern of HAp polycrystals, and the composite characterized the similar nanostructured architecture to native bone. HAp nanocrystals grow on

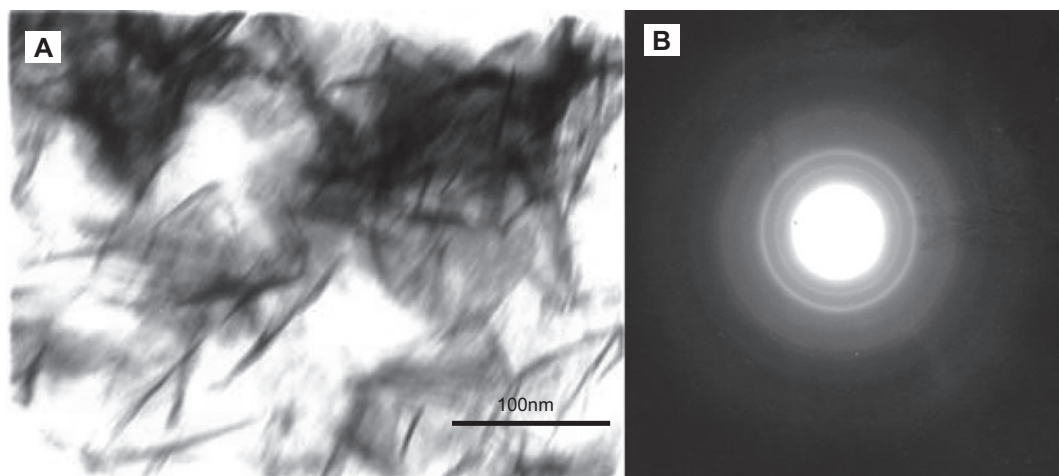


Figure 3 (A) TEM photo of HAp/Col-48 composite; (B) electron diffraction graphic of HAp/Col-48 composite.

Col fibrils in a preferred orientation but the mineralized Col fibrils aggregated to bulk composite randomly revealing a shorter-range ordered but a longer-range disordered structure. In certain conditions, especially the drying method and drying time, oriented Col/HAp nanocomposites materials can be obtained, starting from Col and HAp precursors, through a very simple and accessible *in vitro* modified mineralization method [12]. In a fibril, the molecular level interactions at the interface between molecular Col and HAp nanocrystals have a significant role on its mechanical response [15].

3.4. FT-IR analysis of HAp/Col composite

Figure 4 exhibits the FT-IR spectrum and the zoom-in figures of Col before and after mineralization. Figure 4A gives the comparative IR diagram of pure rat tail Col (plot a) and the as-prepared HAp/Col composite (plot b), which demonstrates the existence of absorption bands originating from vibration of function groups PO_4^{3-} in HAp and amino ($-\text{NH}_2$) in Col, it should be noted that absorption band of the hydroxyl ($-\text{OH}$) is indistinctive, partially due to the effects of large amounts of structural water or the bone-like apatite generated by the substitution of CO_3^{2-} for $-\text{OH}$; additionally, the other possible

reason correlates to the shielding of lattice position of OH^- by PO_4^{3-} . It can be inferred from the spectrum that structure of Col changed owing to mineralization as follows. Firstly, position of absorption peaks of most of the function groups in Col shift to lower wavelengths indicating a physical and chemical interaction between HAp and Col by mineralization, for instance, the stretching vibration peaks of amino and hydroxyl group shift from 3442 to 3427 cm^{-1} , the absorption band of carboxyl ($-\text{COO}^-$) at 1340 cm^{-1} shifts to a position with a lower wavelength, implying the occurrence of chemical interaction and tight bonding between HAp and Col fibrils. Secondly, as depicted in Figure 4C the intensities of three amide absorption peaks decrease, one at 1240 cm^{-1} nearly disappears and one at 1635 cm^{-1} red-shifts to 1659 cm^{-1} because chemical reactions that HAp crystallized and grew on Col had taken place. Ca^{2+} can coordinate with either carboxyl or carbonyl groups in Col; the crystallization and growth of HAp on these two sites enclose carboxyl and carbonyl groups into crystallite, as a result the vibration of carbonyl is hindered without generating IR light, the intensity of amide III thus reduces to nearly perceptible. Additionally, Ca^{2+} coordinating with carbonyl attenuates $\text{C}=\text{O}$ bond resulting in an increased vibration wavelength and red-shift for amide I. Thirdly,

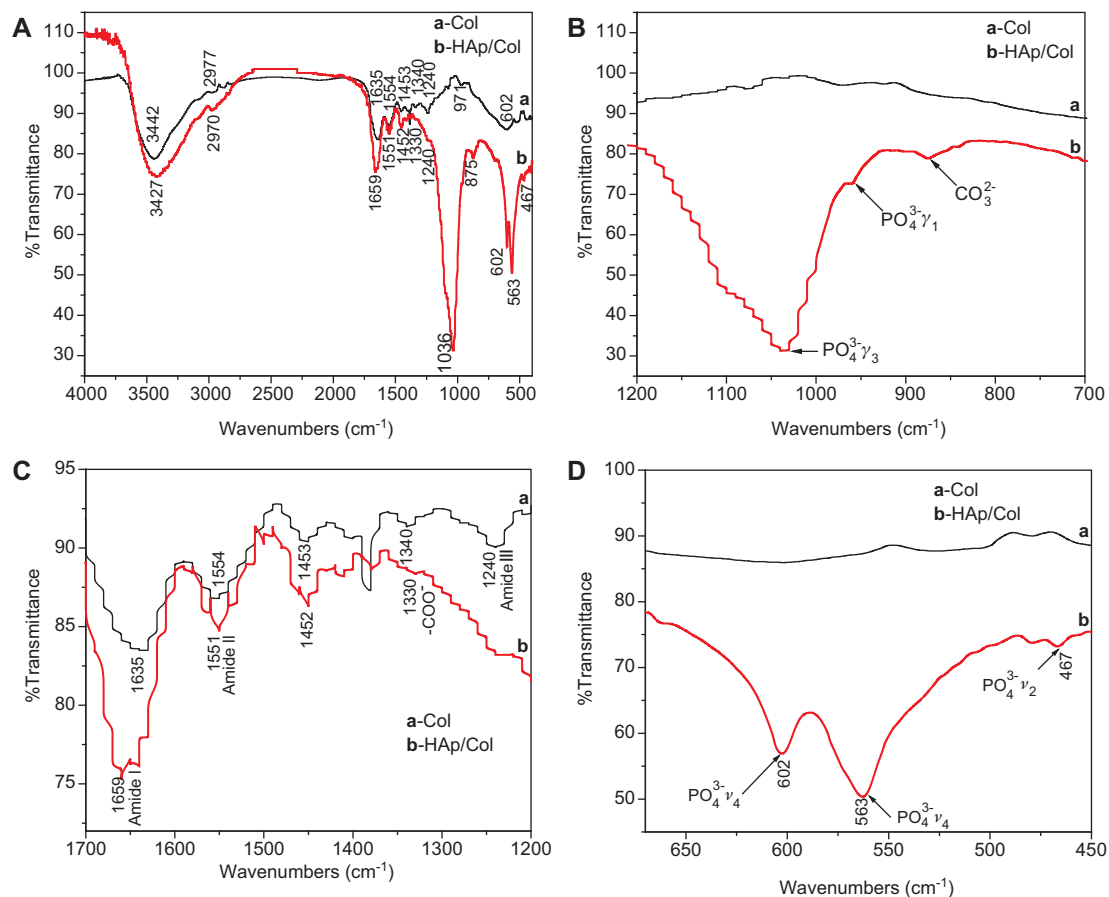


Figure 4 Comparative analysis of FT-IR spectra of Col and HAp/Col. (A) Spectrum for wavelength range of 400–4000 cm^{-1} ; (B) zoom-in spectrum for wavelength range of 700–1200 cm^{-1} ; (C) zoom-in spectrum for wavelength range of 1200–1700 cm^{-1} ; (D) zoom-in spectrum for wavelength range of 450–670 cm^{-1} .

Figure 4B indicates that CO_3^{2-} absorption band appears at 875 cm^{-1} , showing that the inorganic phases carbonated as native bone usually do so during HAp nucleation and growth on Col. As seen in Figure 4D, a strong PO_4^{3-} absorption peak appears at 1036 cm^{-1} in addition to other average PO_4^{3-} absorption peaks at 963 cm^{-1} , 602 cm^{-1} , 563 cm^{-1} , and 467 cm^{-1} , respectively, which also illustrate fine HAp formed and grew on Col fibrils.

3.5. Thermal analysis of HAp/Col

Figure 5 exhibits the thermal analysis plots of HAp/Col including TGA and differential scanning calorimetry (DSC), in which the DSC displays three thermodynamic processes: the mass loss 9.75% revealed by TG plot from room temperature to 150°C indicates a dehydration course of HAp/Col implying a water content of 9.75% of HAp/Col, which is very close to that of pure Col (ca. 10%). The Col in the composite decomposes followed by carbonating when the composite is heated from 324.6°C to 571.1°C , and then the carbonated organics begin to burn when it is continually heated to 712.4°C . The total percentage of organic substance in the composite approaches 12% and the organic substance is added up to be 22% taking into account the bound water content, and thus leaves the inorganic components as 78% or so, which is close to the mass ratio of inorganic to organic phase for native bone. This result demonstrates the successful composition-based imitation of HAp/Col composite to native bone. However, the mass ratio of components in the composite may vary much ascribing to different dosages of Col and HAp starting materials.

4. Discussion

Self-assembled biomaterials are characterized by three common features as: the materials are highly organized at all length scales, they preserve the analogous functional shape or form to the living organism, and possess the sophisticated microstructure even down to the atomic level, the materials are synthesized under benign condition, and the synthesis is

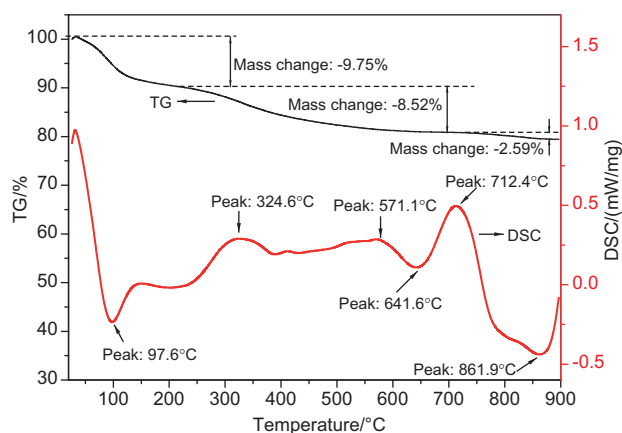


Figure 5 TG and DSC plot of as-prepared HAp/Col composite.

directed and controlled by self-assembled functional molecules. As mentioned above, the self-assembly course of bone formation can be considered conceptually as two aspects: one is the self-assembly of hierarchical structure in Col matrix, and the second involves spontaneous nucleation of Ca/P ions and the oriented array of formed HAp crystals on Col template.

Provided with a condition of stimulated physiological environment, it is assumed that the strong chemical interaction between COO^- groups on the side chains of the trihelix structure of Col molecules and Ca^{2+} from HAp nanocrystals directly nucleate HAp nanocrystals and lead to their preferentially oriented growth with crystalline c-axis parallel to Col fibril axis via a self-assembling process. HAp commences its growth to be nanocrystals with regular orientation and poor crystallization, and furthermore the mineralized Col fibrils progressively organize to be a hierarchical configuration. The morphology shown in Figure 2 exhibits evidence that the hierarchical microstructure of HAp/Col was constructed by self-assembly at multiple levels, the benign reaction condition demonstrates that the biomineralization process was accomplished in a spontaneous manner that leaves out particular exotic intervention.

In such a biomimetic physiological environment, calcium phosphorus salt mineralizes and nucleates directly on the Col molecules templates through self-assembly. HAp crystals are oriented in the c-axis direction parallel to the long axis of the Col fibril via electrostatic interactions between the lateral COO^- in the triple helix structure of Col and Ca^{2+} in the surface of HAp. This evidence for self-assembly of HAp on Col templates is corroborated by the highlighted (211) XRD peak and FT-IR measurements of relative functional groups interactions in Figure 4. The electron bonding state of Ca appears as coordinating bonds with two PO_4^{3-} in HAp and COO^- on Col molecule, respectively. The binding energy of $[\text{Ca}^{2+}\text{-COO}^-]$ is higher than that of $[\text{Ca}^{2+}\text{-PO}_4^{3-}]$, because the organic bond combines the characteristics of ionic and covalent bonds. The coordination between Ca^{2+} and COO^- impairs double bond $\text{C}=\text{O}$ and in turn strengthens Ca-O , and thereby makes COO^- on Col to be the particularly active site to bond with Ca^{2+} yielding ionic compound, which further reacts with PO_4^{3-} to form a critical-sized crystalline nucleus followed by growing to regularly oriented nanocrystals, and the mineralized Col fibrils progressively assemble to be hierarchical structural composites.

5. Conclusions

HAp/Col biomimetic nanocomposite was prepared through self-assembly by a simplified fabrication approach and accessible materials. HAp nanocrystals formed as preferentially oriented slender needles 50–100 nm in length on a felt-like Col matrix which is composed of large numbers of randomly oriented Col fibers and showed polycrystalline behavior. The as-prepared cellular composite is analogous in both composition and nanostructured architecture to native bone, longer aging time promotes the growth and purification of nano-HAp

on Col, and characterization confirms that chemical interaction occurs and causes intimate bonding between HAp and Col. The novel materials have the potential of application in bone substitution grafts and tissue engineering by virtue of its similarities to native bone.

References

- [1] Wahl DA, Czernuszka JT. *Eur. Cells Mater.* 2006, 11, 43–56.
- [2] O'Brien FJ. *Mater. Today* 2011, 14, 88–95.
- [3] Stevens MM. *Mater. Today* 2008, 11, 18–25.
- [4] Kyle S, Aggeli A, Ingham E, McPherson MJ. *Trends Biotechnol.* 2009, 27, 423–433.
- [5] Zhang L, Tang P, Xu M, Zhang W, Chai W, Wang Y. *Acta Biomater.* 2010, 6, 2189–2199.
- [6] Zhai Y, Cui FZ. *J. Cryst. Growth* 2006, 291, 202–206.
- [7] Luo DM, Sang L, Wang XL, Xu SM, Li XD. *Mater. Lett.* 2011, 65, 2395–2397.
- [8] Liu CZ. *J. Bionic Eng.* 2008, Suppl., 1–8.
- [9] Kikuchi M, Koyama Y, Edamura K, Irie A, Sotome S, Itoh S, Takakuda K, Shinomiya K, Tanaka S. In *Advances in Nanocomposites-Synthesis, Characterization and Industrial Applications*. InTech: Croatia, 2011, pp. 181–194.
- [10] Hsu FY, Chueh SC, Wang YJ. *Biomaterials* 1999, 20, 1931–1936.
- [11] Pins GD, Silver FH. *Mater. Sci. Eng.* 1995, C3, 101–107.
- [12] Fikai A, Andronescu E, Voicu G, Ghitulica C, Vasile BS, Fikai D, Trandafir V. *Chem. Eng. J.* 2010, 160, 794–800.
- [13] Olszta MJ, Cheng XG, Jee SS, Kumar R, Kim YY, Kaufman MJ, Douglas EP, Gower LB. *Mater. Sci. Eng.* 2007, R58, 77–116.
- [14] Rhee SH, Suetsugu Y, Tanaka J. *Biomaterials* 2001, 22, 2843–2847.
- [15] Katti DR, Pradhan SM, Katti KS. *J. Biomech.* 2010, 43, 1723–1730.